CALANet: Cheap All-Layer Aggregation for Human Activity Recognition

Jaegyun Park[1], **Dae-Won Kim**[1,*], **Jaesung Lee**[2,*]
[1]School of Computer Science and Engineering, Chung-Ang University, Republic of Korea
[2]Department of Artificial Intelligence, Chung-Ang University, Republic of Korea
`jgp0566.cau@gmail.com`, `{dwkim, curseor}@cau.ac.kr`

Abstract

With the steady growth of sensing technology and wearable devices, sensor-based human activity recognition has become essential in widespread applications, such as healthcare monitoring and fitness tracking, where accurate and real-time systems are required. To achieve real-time response, recent studies have focused on lightweight neural network models. Specifically, they designed the network architectures by restricting the number of layers shallowly or connections of each layer. However, these approaches suffer from limited accuracy because the classifier only uses the features at the last layer. In this study, we propose a cheap all-layer aggregation network, CALANet, for accuracy improvement while maintaining the efficiency of existing real-time HAR models. Specifically, CALANet allows the classifier to aggregate the features for all layers, resulting in a performance gain. In addition, this work proves that the theoretical computation cost of CALANet is equivalent to that of conventional networks. Evaluated on seven publicly available datasets, CALANet outperformed existing methods, achieving state-of-the-art performance. The source codes of the CALANet are publicly available at `https://github.com/jgpark92/CALANet`.

1 Introduction

Human activity recognition (HAR) is a fundamental technique in healthcare [28, 53], fitness tracking [5, 23], and surveillance [21, 41]. Wearable sensor-based HAR has drawn attention in pervasive computing applications due to the popularity of smart wearable devices in recent years [7, 53]. Specifically, it aims to identify motion details of users or activity tracks from sensor signal patterns [10]. To this end, neural networks (NNs) have been widely used to achieve a superior learning performance without handcrafted feature engineering [7, 52]. Besides, with advances in microelectronics and inertial sensor-based wearable devices, recent researchers have focused on achieving real-time systems [4, 43]. Especially, a recent trend across most studies has become increasingly to train NNs on a resource-rich computing device and then deploy them to resource-limited wearable devices, where inference is executed [44, 60, 61].

Recent real-time HAR studies have focused on one-dimensional (1D) convolutional neural networks (CNNs) compatible with various hardware accelerators and deployment frameworks [14, 20, 23, 36, 37, 48, 51, 60]. CNNs include convolution and pooling operations, which allow them to extract more abstracted high-level features as input signals pass from early to later layers. Specifically, the pooling operation abstracts signals by reducing the feature size (temporal resolution), which can be regarded as a sampling of signal. As a result, the final classifier predicts an activity class based on the abstracted or sampled features at the last layer. The sampled features are more semantic and global

*Corresponding authors.

38th Conference on Neural Information Processing Systems (NeurIPS 2024).

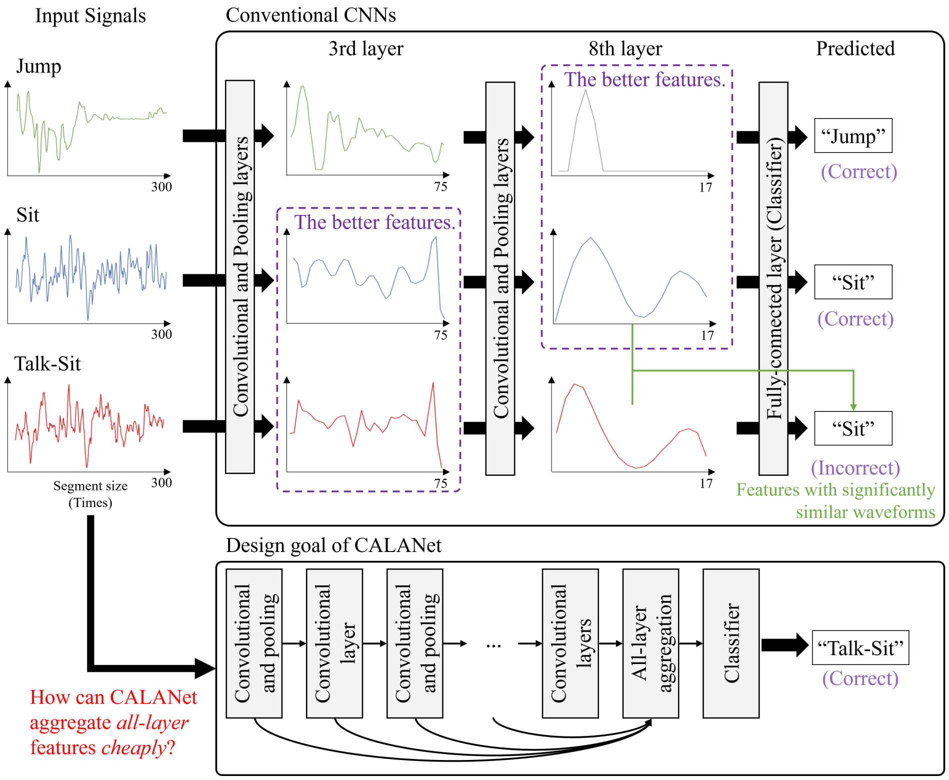

Figure 1: Analysis of representations in our experiments on KU-HAR dataset [47]. In a conventional CNN, the classifier predicts activities only using the feature representations at the last layer. Features at the early layer include the detailed information of original signals that may confound the classifier. In comparison, features at the later layer are more semantic, but the features (with more compact and short waveforms) make it challenging to classify activities that share similar semantics. Our goal is to design a CALANet that allows the classifier to use features for all layers while maintaining the inference time of conventional CNNs.

than those of prior layers, but it has not been proven that the last layer is the optimal representation [58]. Although the high-level features sampled by the pooling operation can avoid over-fitting of the classifier [59], for the HAR dataset, the loss of some detailed information makes it challenging to classify activities that share similar semantics, such as "Sit" and "Talk-Sit."

Figure 1 illustrates intermediate features in the forward pass of conventional CNNs. Conventional CNNs classify "Jump" and "Sit" well but tend to misclassify "Talk-Sit" as another activity, as shown in Figure 1. These experimental observations have also been reported in existing studies [24, 47]. Specifically, the features at the eighth layer (with more compact and short waveforms) make it easy for the classifier to discriminate "Jump" and "Sit," compared with the ones at the third layer. On the contrary, the features at the third layer (with more detailed information) can be more suitable than the ones at the eighth layer when classifying "Sit" and "Talk-Sit" that have similar vibrations in signal waveforms. Although which layer has the best features depends on the activity, conventional CNNs classify multiple activities only using the features at the last layer.

The objective of real-time HAR is to maximize accuracy under real-time constraints. To achieve real-time response, prior HAR studies designed the network architectures of CNNs by restricting the number of layers shallowly [20, 23, 51, 60] or reducing connections of each layer [14, 36, 37, 48]. However, these approaches suffer from limited accuracy because their classifier only uses the features at the last layer. A straightforward approach to address this issue is to allow the classifier to use the features for all layers [19, 27], but this leads to a substantial increase in computational cost, particularly as the number of layers deepens. Therefore, our goal is to design a novel network architecture that allows the network to aggregate the features for all layers *while maintaining the computational cost of the conventional CNNs regardless of network depth*, as shown in Figure 1.

In this paper, we propose a novel network, CALANet, with a cheap *all-layer* aggregation (CALA) structure. To achieve our goal, CALANet includes (1) learnable channel-wise transformation matrices and (2) scalable layer aggregation pool. First, we introduce new learnable channel-wise transformation matrices (LCTMs) to minimize an increase in computational cost due to all-layer aggregation. Given intermediate features at a specific layer (with temporal resolution T and the number of channels M), M LCTMs generate a vector with $N \ll T$ elements based on linear transformation and combination without increasing the theoretical computation cost. Second, we improve the effectiveness of all-layer aggregation by introducing a scalable layer aggregation pool (SLAP) that allows CALANet to stack layers without significantly increasing computational costs. As a result, the main contributions of this paper are as follows:

- We proposed CALANet with a CALA structure that allows the network to aggregate the features for all layers while maintaining the efficiency of CNNs regardless of network depth based on (1) LCTMs and (2) SLAP.
- We theoretically proved that the computational cost of CALANet is equivalent to that of conventional CNNs, including even shallow networks.
- We empirically demonstrated the effectiveness of CALANet in achieving superior performance compared to 11 state-of-the-art methods on seven public benchmark datasets.

2 Related Work

Many comprehensive surveys in HAR literature have highlighted the importance of NN-based models and real-time applications [7, 10, 34, 42–44, 52, 61]. For instance, early real-time HAR studies adopted two-dimensional (2D) convolutional NNs (CNNs) with shallow architectures [9, 25, 33, 45]. Specifically, they transformed the sensor signal patterns to 2D spectral images as an input of 2D CNNs. However, these approaches require complex preprocessing, such as discrete or short-time Fourier transform, which increases the overhead during continuous processing for real-time HAR. Meanwhile, Ignatov [23] proposed a one-dimensional (1D) CNN architecture using basic statistical features to encode global temporal information. Although this approach demonstrated the potential of 1D CNN, it still requires several data preprocessing like calculating the histogram of input signals.

Recent real-time HAR studies focus on 1D CNNs without any complex data preprocessing. For example, Zebin et al. [60] proposed a CNN architecture comprising four convolution layers. Furthermore, they showed the efficiency of parameter quantization as post-processing for further optimization. In another study, Wan et al. [51] adopted a CNN architecture including three convolution layers. They demonstrated the superiority of CNNs compared with recurrent NN variants on HAR datasets with basic activities. To enhance shallow CNNs, Huang et al. [20] introduced a cross-channel communication that exchanges information among channels within the same layer. These models achieved real-time HAR by shallowly restricting the number of layers, resulting in limited accuracy.

To alleviate the issue, some studies have considered efficient variants of convolution at each layer instead of reducing the number of layers. For example, Gao et al. [14] proposed a selective kernel module that divides the convolution into split, fuse, and select steps to adjust receptive field size adaptively. Similarly, Tang et al. [48] designed a hierarchical-split block to enhance multiscale temporal features by composing channel groups hierarchically. In another study, Teng et al. [49] proposed RepHAR, which re-parameterizes a pretrained multibranch CNN to a plain CNN before deploying it into resource-limited devices. However, these approaches still are insufficient to classify activities that have similar vibrations in signal waveforms because the classifier only uses the features at the last layer. Meanwhile, Park et al. [37] introduced a grouped temporal shift network that can flexibly re-design a network architecture to support various hardware specifications. Although this network can derive layer-specific structures suitable for a given computational budget, its performance is limited according to an initial network architecture. Therefore, its performance can be improved by using our CALANet as the initial network, as will be described in Section 4.2.

Besides, the classifier requires both local and global temporal representations to achieve high HAR accuracy [64]. Specifically, the locality of CNNs improves accuracy due to their translational invariance concerning the precise location of activity within a segment of time-series data [17]. On the other hand, recurrent layers or attention mechanisms have an advantage for global feature extraction because they can model long-term dependencies. In this regard, many studies have attempted to integrate recurrent layers [8, 24, 35, 50, 56] or attention mechanisms [40, 63] into

CNNs, which has increased both accuracy and inference times. The increase in inference time is primarily because of the lack of device-level optimizations compared with CNNs [15, 29, 60]. These accuracy-oriented networks will be compared with our CALANet in Section 4.2.

3 Cheap All-Layer Aggregation Network

In this section, our goal is to design a CNN architecture that can aggregate features for all layers into the final classifier without increasing the computational cost of CNNs. Furthermore, we prove that the theoretical computation cost of the proposed CALANet is equivalent to that of conventional CNNs, including even shallow networks.

3.1 Computational cost of convolutional neural networks

Our goal is to improve the HAR accuracy while maintaining the efficiency of CNNs. Therefore, before deriving a novel network structure and proving its theoretical efficiency, we formalize the computational cost of the conventional CNNs in a generalized form. Note that we only consider the computational cost in the feed-forward step, not the training step, which is unrelated to inference time. Let $\mathcal{K}^{(l)}$ be the l-th layer of a network, where $\mathcal{K}^{(l)}$ and $\mathcal{K}^{(l+1)}$ are calculated sequentially and independently. Therefore, the theoretical computation cost of the CNN can be defined as a summation for each computation of layers, as described in Definition 1.

Definition 1. *Let $\alpha(\cdot)$ be the computational cost of calculating the output of each layer. Given a network architecture $\mathcal{A}$ with L layers, the input $X^{(l)}$ is fed into the l-th layer with trainable parameters $\theta^{(l)}$ to calculate the output $X^{(l+1)}$. Due to this layer composition, its computational cost is formalized as*

$$C_n(\mathcal{A}) = \sum_{l=1}^{L} \alpha(\mathcal{K}^{(l)}(X^{(l)}; \theta^{(l)})). \tag{1}$$

To formalize the computation cost of CNNs, we borrow the concept of time complexity as the upper bound of the computational cost. Similar to Proposition 3 of [37], Eq. (1) is simplified by Proposition 1.

Proposition 1. *The time complexity of CNNs is formalized as:*

$$\mathbb{M} \leq \mathbb{N}(L-1) \Longrightarrow \mathcal{O}(\mathbb{T}\mathbb{D}_k\mathbb{N}^2 L). \tag{2}$$

where $\mathbb{M}$ and $\mathbb{T}$ are the number of channels and temporal resolution for input data, and $\mathbb{N}$ and $\mathbb{D}_k$ are average numbers for output channels and kernel sizes across a network, respectively.

The proof is given in Appendix A. Because we do not restrict the number of layers shallowly, we will assume that the condition of Eq. (2) is always true in this paper.

3.2 Learnable channel-wise transformation matrix

In this section, we introduce a learnable channel-wise transformation matrix (LCTM) that allows our CALANet to aggregate features for all layers without increasing the theoretical computation cost. Figure 2 shows the network architecture of CALANet. Given input signals, the convolution and pooling layers extract the high-level sampled features by calculating temporal correlations and reducing the feature resolution. After that, the features for all layers are connected with the classifier via the cheap all-layer aggregation module based on the LCTMs.

Let $\mathbf{x_m}$ be a feature vector of m-th channel with temporal resolution $T = |\mathbf{x_m}|$ at any layer. Because T varies with the layer, we define a mapping function $f : \mathbf{x_m} \rightarrow \mathbf{y} \in \mathbb{R}^N$, where a constant value $N \ll T$. After that, we calculate f via a transformation matrix $\mathbf{A} \in \mathbb{R}^{N,T}$. As the mapping function is calculated for each channel of features, m-th feature vector is transformed to $\mathbf{y_m} \in \mathbb{R}^N$ as follows:

$$\mathbf{y_m} = \mathbf{A_m}\mathbf{x_m} \tag{3}$$

where this transformation can be interpreted as a compression of global temporal information. After that, a linear combination is conducted to calculate relations between channels as follows:

$$\hat{\mathbf{y}} = \sum_m a_m \mathbf{y_m} \tag{4}$$

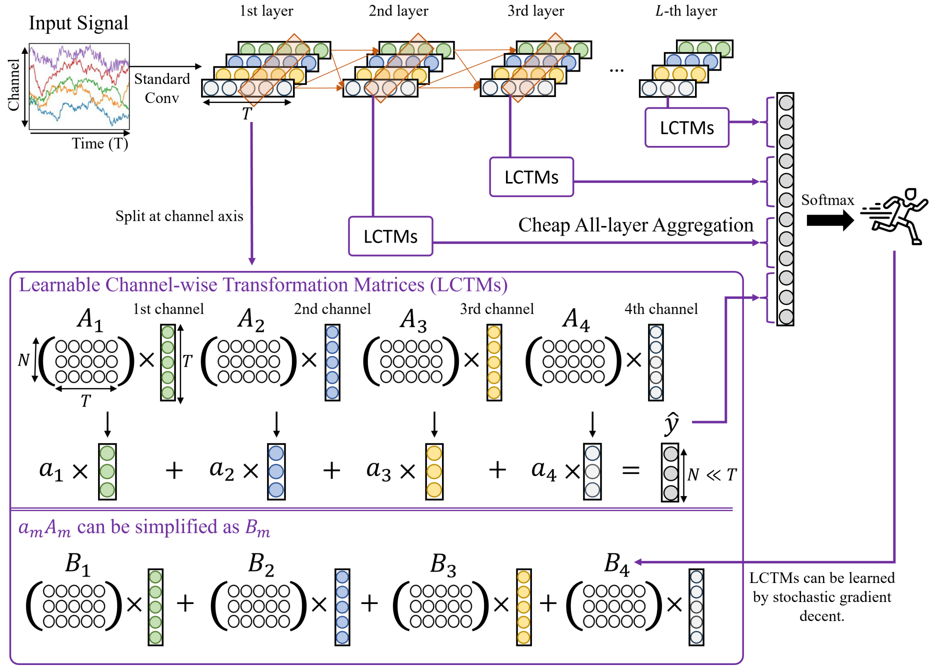

Figure 2: Network architecture of CALANet. Convolution and pooling layers extract the sampled features by reducing the temporal resolution. CALANet aggregates the features for all layers based on the linear transformation and combination.

where $\hat{\mathbf{y}} \in \mathbb{R}^N$ is a vector and a_m is m-th coefficient of the linear combination.

We replace $a_m\mathbf{A_m}$ with $\mathbf{B_m} \in \mathbb{R}^{N,T}$. As a result, Eq. (4) is simplified as follows:

$$\hat{\mathbf{y}} = \sum_m \mathbf{B_m}\mathbf{x_m} \tag{5}$$

where elements of $\mathbf{B_m}$ can directly be optimized by stochastic gradient descent because these matrix multiplications can be implemented by dense layers. Therefore, we define B_m as LCTM. Herein, the time complexity of calculating M LCTM operations is $\mathcal{O}(TMN)$. Finally, $\hat{\mathbf{y}}$ for all layers are concatenated and then fed into the classifier.

To investigate whether our CALANet can maintain the efficiency of conventional CNNs, we analyze the time complexity of CALANet. Based on Proposition 1, the time complexity of CALANet is formalized in Lemma 1.

Lemma 1. *The time complexity of CALANet is equivalent to:*

$$\mathcal{O}(\mathbb{T}\mathbb{D}_k\mathbb{N}^2L). \tag{6}$$

The proof is given in Appendix B. According to Proposition 1 and Lemma 2, our CALANet can aggregate features for all layers while maintaining the efficiency of conventional CNNs.

3.3 Scalable layer aggregation pool

The effectiveness of all-layer aggregation depends on a layer aggregation pool, i.e., the number of layers, as shown in Table 3. To improve the accuracy of CALANet further, we also introduce a scalable layer aggregation pool (SLAP) that allows CALANet to stack layers without significantly increasing computational cost. To this end, we, in this section, aim to omit L in Eq. (2). Inspired by ShuffleNet [62], we first use the grouped convolution and channel shuffle to reduce the time complexity of the standard convolutions. Precisely, the M input channels are evenly divided into G channel groups. After that, the standard convolution generates $\lfloor N/G \rfloor$ output channels for each channel group. Subsequently, the channel shuffle operation is executed.

The entire channels are fully related by the channel shuffle operations if and only if (the number of layers) $\times$ (the number of channels within each channel group) $\geq$ (the number of channel groups) [62]. Therefore, G is set into a value satisfying $L \times N \geq G^2$. As $N \geq G$ and G are inversely proportional to the computational cost, we set G into L without any loss of information for channel correlations. Consequently, the time complexity of the stack of the standard convolutions is reduced in Lemma 2.

Lemma 2. *The time complexity of calculating the standard convolutions is reduced to:*

$$\mathcal{O}(\mathbb{T}\mathbb{D}_k\mathbb{N}^2). \tag{7}$$

The proof is given in Appendix C. To reduce the time complexity of all-layer aggregation, we focus on the norm of vectors extracted from LCTMs, i.e., $|\hat{\mathbf{y}}| \approx \mathbb{N}$ from Eq. (5). The LCTMs for all layers generate a vector with $L \times \mathbb{N}$ elements fed into the Softmax layer to classify the activities. The large number of units in the Softmax layer may incur overfitting [57]. Therefore, we fix the number of features fed into the Softmax layer to $\mathbb{N}$ by dividing the number of rows of LCTM in Eq. (5) by L, resulting in $\mathbf{B_m} \in \mathbb{R}^{N/L,M}$. Consequently, the time complexity of all-layer aggregation is reduced in Lemma 3.

Lemma 3. *The time complexity of calculating all-layer aggregation is formalized as:*

$$\mathcal{O}(\mathbb{T}\mathbb{N}^2). \tag{8}$$

The proof is given in Appendix D. Finally, we introduce CALANet with the SLAP by omitting the factor L from its time complexity. Consistent with Lemma 2 and Lemma 3, the time complexity of CALANet is reduced in Theorem 1.

Theorem 1. *The time complexity of CALANet is reduced to:*

$$\mathcal{O}(\mathbb{T}\mathbb{D}_k\mathbb{N}^2). \tag{9}$$

The proof is given in Appendix E. From Theorem 1, we crosscheck the efficiency of our CALANet by making comparisons with the time complexity of shallow CNNs in Corollary 1 and Corollary 2.

Corollary 1. *The time complexity of CALANet is equivalent to the shallow CNNs with $L \geq 2$.*

Proof. The time complexity of shallow CNNs with $L = 2$ is $\mathcal{O}(\mathbb{T}\mathbb{D}_k\mathbb{M}\mathbb{N}) + \mathcal{O}(\mathbb{T}\mathbb{D}_k\mathbb{N}^2) = \mathcal{O}(\mathbb{T}\mathbb{D}_k\mathbb{N}^2)$. It is equivalent to Eq. (9). ☐

Corollary 2. *The time complexity of CALANet is equivalent to the shallow CNNs with $L = 1$ if $\mathbb{M} \approx \mathbb{N}$.*

Proof. The time complexity of shallow CNNs with $L = 1$ is $\mathcal{O}(\mathbb{T}\mathbb{D}_k\mathbb{M}\mathbb{N})$. If $\mathbb{M} \approx \mathbb{N}$, then it is equivalent to Eq. (9). ☐

In conclusion, our CALANet has a computation cost comparable to shallow CNNs. Especially from Corollary 2, the time complexity of CALANet becomes equivalent to the shallow CNNs even with $L = 1$ as the number of sensors increases.

4 Experiments

In this section, we evaluate the superiority of CALANet. In Section 4.1, we describe the experimental setup. Section 4.2 presents the compared results of CALANet and other networks on seven HAR datasets. Section 4.3 provides an in-depth analysis via an ablation study. Lastly, Section 4.4 measures the actual inference time of CALANet.

4.1 Experimental Settings

Dataset. We used seven public benchmark datasets, including various sampling frequencies, the number of activities, and sensors. They include **UCI-HAR** [1], **UniMiB-SHAR** [30], **DSADS** [3], **OPPORTUNITY** [6], **KU-HAR** [47], **PAMAP2** [46], and **REALDISP** [2]. The details for each dataset are described in Appendix F.

Table 1: Comparison results on seven datasets. ▼/△ indicates that the corresponding model is significantly worse/better than CALANet according to a paired t-test at a 95% significance level.

	UCI-HAR		UniMiB-SHAR		DSADS		OPPORTUNITY	
Model	F1	FLOPs	F1	FLOPs	F1	FLOPs	F1	FLOPs
CALANet (**Ours**)	96.1	**7.6M**	78.3	**8.8M**	90.0	**8.5M**	81.6	**19.3M**
CALA-GTSNet (**Ours**)	94.7▼	3.3M	74.1▼	4.8M	87.2▼	5.4M	78.4▼	15.0M
Shallow ConvNet [23]	92.5▼	17.9M	72.2▼	18.2M	85.6▼	48.5M	79.5▼	74.3M
RepHAR [49]	95.1▼	31.8M	71.6▼	37.3M	85.5▼	32.9M	80.0▼	26.0M
Res-GTSNet [37]	94.5▼	6.4M	77.2▼	7.51M	84.4▼	7.3M	76.0▼	6.4M
DeepConvLSTM [35]	91.4▼	67.2M	71.6▼	80.4M	85.5▼	68.3M	62.0▼	50.4M
Bi-GRU-I [50]	94.6▼	46.1M	75.2▼	54.0M	85.6▼	48.7M	77.2▼	39.8M
RevAttNet [40]	95.1▼	143.1M	76.7▼	168.7M	87.6▼	140.2M	78.6▼	101.5M
IF-ConvTransformer [63]	95.4	209.8M	77.0▼	183.5M	87.5▼	628.4M	82.2	986.2M
T-ResNet [54, 12]	95.3	123.2M	76.5▼	145.5M	87.3▼	125.8M	80.9	96.9M
T-FCN [54, 12]	95.8	68.9M	76.9▼	80.6M	86.7▼	76.1M	76.2▼	65.8M
MILLET [11]	94.7▼	111.6M	81.4△	129.9M	84.3▼	132.8M	82.3	125.0M
DSN [55]	95.4	270.8M	79.8	320.0M	86.4▼	265.7M	71.8▼	192.1M

	KU-HAR		PAMAP2		REALDISP	
Model	F1	FLOPs	F1	FLOPs	F1	FLOPs
CALANet (**Ours**)	97.5	**29.6M**	79.4	**74.9M**	98.2	**56.7M**
CALA-GTSNet (**Ours**)	96.1▼	12.2M	76.3▼	23.9M	95.4▼	43.3M
Shallow ConvNet [23]	77.9▼	41.6M	67.4▼	151.8M	95.9▼	209.9M
RepHAR [49]	93.4▼	74.4M	73.0▼	131.9M	94.7▼	72.7M
Res-GTSNet [37]	94.5▼	15.3M	76.2▼	28.6M	94.9▼	18.0M
DeepConvLSTM [35]	93.5▼	169.1M	77.3▼	303.9M	91.7▼	156.9M
Bi-GRU-I [50]	94.9▼	108.0M	71.0▼	194.1M	96.1▼	111.3M
RevAttNet [40]	97.7	335.3M	79.7	573.5M	98.5	282.1M
IF-ConvTransformer [63]	96.4▼	491.7M	80.1	1.7G	97.4	3.0G
T-ResNet [54, 12]	95.0▼	290.0M	71.4▼	506.1M	96.0▼	270.1M
T-FCN [54, 12]	92.5▼	161.7M	72.5▼	298.5M	95.9▼	184.5M
MILLET [11]	97.8	262.5M	80.2	509.5M	95.1▼	352.9M
DSN [55]	97.1	634.8M	68.8▼	1.08G	97.5	532.7M

Baseline. We compared CALANet with 11 baseline networks. To evaluate the efficiency of CALANet, we used Shallow ConvNet [23], RepHAR [49], and Res-GTSNet [37] as state-of-the-art models in real-time HAR. Meanwhile, we adopted four CNNs with recurrent layers or attention mechanisms, including DeepConvLSTM [35], Bi-GRU-I [50], RevAttNet [40], and IF-ConvTransformer [63], to verify the effectiveness of our all-layer aggregation. In addition, we used four networks, T-ResNet [54, 12], T-FCN [54, 12], MILLET [11], and DSN [55] that achieved substantial success in the time-series classification (TSC), which is more general-purpose than HAR. The details for the models and hyperparameters are described in Appendix G.

To evaluate the performance of CALANet, we used two metrics: F1-score and floating-point operations (FLOPs). Because the HAR datasets inherently involve a class imbalance, the F1-score has been commonly used as an alternative for accuracy. In particular, FLOPs have been widely used to describe how many operations a given model requires to run a single pattern. In addition, we investigate the change in performance according to L, as will be described in Section 4.3. Meanwhile, Res-GTSNet [37] can derive layer-specific structures suitable for a given computational budget, and the original paper adopted T-ResNet as an initial network. To improve the efficiency of CALANet further, we also designed the CALA-GTSNet by replacing T-ResNet with our CALANet.

4.2 Comparison results

Table 1 shows the results of comparing CALANet and the baseline networks. The experiments ran ten times, and the average values were recorded on all the datasets. In addition, we performed a paired

Table 2: Ablation study of CALANet on two datasets; LCTMs: Learnable channel-wise transformation matrices, SLAP: Scalable layer aggregation pool, ALA: All-layer aggregation

		KU-HAR		PAMAP2	
Networks	L	F1	FLOPs	F1	FLOPs
CALANet with LCTMs + SLAP	9	97.5	29.7M	79.4	74.9M
CALANet with LCTMs only	4	93.8▼	60.0M	73.1▼	113.3M
CALANet with ALA only	4	95.0▼	577.9M	72.8▼	1.7G

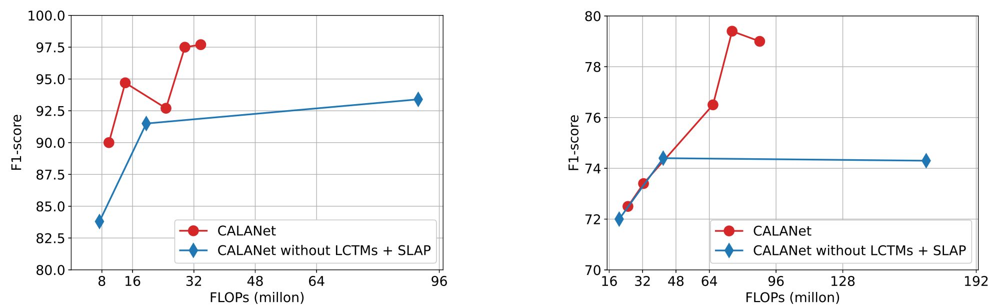

(a) KU-HAR dataset

(b) PAMAP2 dataset

Figure 3: Tradeoff between the FLOPs and F1-score.

t-test at the 95% significance level on each dataset. In Table 1, ▼/△ indicates that the compared network was significantly worse/better than CALALet regarding the F1-score.

Comparison with real-time CNNs. In Table 1, the F1-scores of CALANet were statistically superior to real-time HAR models on all datasets. In particular, CALANet has the lowest FLOPs compared to other real-time HAR models with standard convolution layers on seven datasets. Meanwhile, Res-GTSNet, with an efficient variant of the convolution, exhibited significantly low FLOPs. This variant can be easily integrated with our CALANet to reduce its FLOPs further. As shown in Table 1, CALA-GTSNet outperformed Res-GTSNet on 86% of the datasets. Also, CALA-GTSNet has lower FLOPs than Res-GTSNet on 71% of the datasets. As a result, CALANet and GTSNet can complement each other to improve the accuracy or reduce computations. These results demonstrated that our cheap all-layer aggregation can maintain a low computational cost.

Comparison with accuracy-oriented networks. We noted that real-time or efficient HAR models using wearable sensors process the input signals with short segmentation lengths for rapid response. If CNNs are sufficient to extract meaningful information from the short-term signals, unnecessary increases in inference time due to integration with recurrent layers or attention mechanisms can be avoided. In Table 1, CALANet outperformed two CNNs with recurrent layers, i.e., DeepConvLSTM and Bi-GRU-I, on all datasets. Compared with RevAttNet and IF-ConvTransformer, CALANet exhibited a comparable F1-score despite its significantly low FLOPs. These results indicate that CNNs are sufficient to model the temporal information for the real-time HAR dataset. Compared with TSC models, CALANet showed comparable performance despite its significantly low FLOPs. These results demonstrated that our cheap all-layer aggregation can significantly improve HAR accuracy while maintaining low FLOPs.

4.3 Ablation study

The breakdown effect of CALANet. We conducted an ablation study to investigate the effectiveness and efficiency of our CALANet. The key components of CALANet are LCTMs and SLAP. Therefore, we compared the performance of our CALANet with that of its two variants, which were obtained by removing each component. The first variant removes the SLAP described in Section 3.3. The second variant replaces the LCTMs with fully-connected layers that have the same number of units as the input size. Table 2 shows that our LCTMs substantially reduced the FLOPs for calculating all-layer aggregation without losing the F1-score. In addition, the SLAP enhanced the effectiveness of all-layer

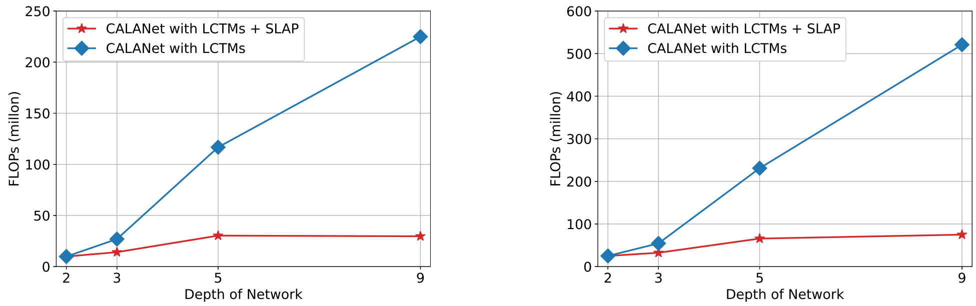

(a) KU-HAR dataset

(b) PAMAP2 dataset

Figure 4: Comparison among two networks with regard to the impact of L on the FLOPs.

aggregation even while reducing FLOPs. Especially, Figure 3 shows the tradeoff between the FLOPs and F1-score with varying numbers of layers in CALANet with/without LCTMs and SLAP. The tradeoff curves closer to the top-left are more efficient, with a higher F1-score per FLOPs. As shown in Figure 3, CALANet with LCTMs and SLAP achieved a higher F1-score in similar computational cost than one without LCTMs and SLAP.

Effect of scalable layer aggregation pool. We investigated the layer aggregation pool at which the best F1-score of CALANet is achieved on seven datasets. Table 3 shows the change in F1-score of CALANet as the layer aggregation pool L increased; herein, the best F1-score is indicated by the bold font on each dataset. As shown in Table 3, the layer aggregation pool and F1-score tend to be proportional. In Figure 4, CALANet with SLAP (red line) exhibited a negligible increase in FLOPs compared with CALANet only with LCTMs. As a result, SLAP allows CALANet to stack layers without significantly increasing FLOPs.

Table 3: F1-score of CALANet on different layer aggregation pool, i.e., network depth L

	L				
Datasets	2	3	5	9	17
UCI-HAR	93.2	93.9	94.8	**96.1**	95.7
UniMiB-SHAR	72.8	76.0	78.0	**78.3**	77.5
DSADS	87.2	84.5	86.0	**90.0**	89.4
OPPORTUNITY	78.9	80.2	79.0	**81.6**	80.3
KU-HAR	90.0	94.7	92.7	97.5	**97.7**
PAMAP2	72.5	73.4	76.5	**79.4**	79.0
REALDISP	92.9	96.7	96.9	**98.2**	97.7

Performance analysis on similar activities. To verify the performance of CALANet, we investigated the confusion matrices (see Appendix H). Prior works [47, 24] suffered from activities that have similar vibrations in signal waveforms, such as "Sit" and "Talk-Sit," as described in Section 1. Compared with these works, our CALANet significantly improved the accuracy of those activities on the KU-HAR dataset. For other examples, these activities include ("rope jumping" and "waking") [20, 14, 48, 49] and ("knees bending crouching" and "reach heels backwards") [8]. On the other hand, our CALANet correctly classified "rope jumping" as "waking" compared to RepHAR that misclassified "rope jumping" as "walking" 20 times [49] on the PAMAP dataset. Compared to MG-WHAR [8] misclassified "knees bending crouching" by approximately 20% as "reach heels backwards", our CALANet misclassified "knees bending crouching" as "reach heels backwards" only two times on the REALDISP dataset.

Applicability of CALA structure. Our CALA structure can effectively be applied to existing CNNs if the following constraints are satisfied: (1) the layers of a network architecture should be calculated sequentially and independently; (2) the output of each layer should be able to be expressed as a (temporal length $\times$ channel size) matrix. To the best of our knowledge, most wearable sensor-based human activity recognition models can satisfy the above constraints. In Table 4, we applied our LCTMs and SLAP to SqueezeNet [22]. Specifically, the output of a squeeze convolution layer in each fire module is fed into LCTMs and connected to the last layer. As a result, our modification significantly improved the F1-score of SqueezeNet on 71% of all datasets while maintaining its FLOPs. In addition, we applied CALANet to the ECG heartbeat classification problem using the MIT-BIH arrhythmia dataset [16]. CALANet exhibited comparable performance with other networks

Table 4: Comparison results of SqueezeNet with/without CALA structure on seven datasets.

	UCI-HAR		UniMiB-SHAR		DSADS		OPPORTUNITY	
Model	F1	FLOPs	F1	FLOPs	F1	FLOPs	F1	FLOPs
SqueezeNet + CALA (**Ours**)	92.4	8.2M	75.8	9.5M	87.3	11.4M	68.4	12.3M
SqueezeNet	92.1	10.4M	74.9	12.4M	84.7▼	13.7M	59.7▼	13.2M

	KU-HAR		PAMAP2		REALDISP	
Model	F1	FLOPs	F1	FLOPs	F1	FLOPs
SqueezeNet + CALA (**Ours**)	96.7	19.5M	70.4	41.5M	93.7	34.8M
SqueezeNet	94.5▼	25.5M	68.0▼	52.9M	85.6▼	39.7M

[13, 39] designed to process ECG signals (see Appendix I). This result shows that CALANet has promising applicability to other ML applications.

4.4 Real-Time Activity Prediction

To estimate the actual response time of our CALANet, we used the AMD Ryzen 7 5800X 8-Core Processor without the support of graphics processing units. Particularly, we compared the inference time of CALANet with Shallow ConvNet. Similar to the conventional real-time HAR studies, the measurements were repeated 1,000 times, and the minimum, maximum, and mean values were recorded. Table 5 shows the inference time of the two networks, where the window length was set to 300 (3 *s*) to slide one instance at a time. CALANet exhibited a response time similar to Shallow ConvNet, even though its depth is nine times deeper than that of Shallow ConvNet. Consequently, these measurements show that our model is sufficient to meet the real-time requirements.

Table 5: Actual inference time of CALANet

	Inference Time (ms / window)		
Model	Min	Mean	Max
CALANet	1.59ms	2.25ms	3.40ms
Shallow ConvNet	1.57ms	2.15ms	3.48ms

5 Conclusion

In this article, we proposed an effective neural network called CALANet for real-time HAR from wearable sensors. In particular, our CALANet has an all-layer aggregation structure that can aggregate features for all layers based on the learnable channel-wise transformation matrix and scalable layer aggregation pool. As a result, CALANet improved HAR accuracy while maintaining the efficiency of existing real-time HAR models. In addition, we proved that the computational cost of CALANet is equivalent to that of shallow CNNs. Our experiments demonstrated that CALANet could achieve state-of-the-art performance on the HAR datasets under low latency.

Future studies can be conducted to overcome the limitations of the proposed method. CALANet does not consider the various computational budgets that can be changed according to the specific devices and the runtime optimizations of actual devices, such as memory access costs and parallel computations. For example, future studies may further improve CALANet by introducing a new operator designed to match the target device.

Acknowledgement. This research was supported in part by the Institute of Information & Communications Technology Planning & Evaluation (IITP) grant funded by the Korean Government (MSIT) (2021-0-01341, Artificial Intelligence Graduate School Program (Chung-Ang University)), in part by the Institute of Information & Communications Technology Planning & Evaluation (IITP) grant funded by the Korean Government (MSIT) (2021-0-00766, Development of Integrated Development Framework that supports Automatic Neural Network Generation and Deployment optimized for Runtime Environment), and in part by the National Research Foundation of Korea (NRF) grant funded by the Korea government (MSIT) (No. 2023R1A2C1006745).

References

[1] D Anguita, A Ghio, L Oneto, X Parra, and JL Reyes-Ortiz. A public domain dataset for human activity recognition using smartphones. In *Proc. 21st Int. Eur. Symp. Artif. Neural Netw., Comput. Intell. Mach. Learn. (ESANN)*, pages 437–442, Apr. 2013.

[2] Oresti Baños, Miguel Damas, Héctor Pomares, Ignacio Rojas, Máté Attila Tóth, and Oliver Amft. A benchmark dataset to evaluate sensor displacement in activity recognition. In *Proc. ACM Conf. Ubiquitous Comput.*, pages 1026–1035, Sep. 2012.

[3] Billur Barshan and Murat Cihan Yüksek. Recognizing daily and sports activities in two open source machine learning environments using body-worn sensor units. *Comput. J.*, 57(11): 1649–1667, Nov. 2014.

[4] Valentina Bianchi, Marco Bassoli, Gianfranco Lombardo, Paolo Fornacciari, Monica Mordonini, and Ilaria De Munari. IoT wearable sensor and deep learning: An integrated approach for personalized human activity recognition in a smart home environment. *IEEE Internet Things J.*, 6(5):8553–8562, Oct. 2019.

[5] Andreas Bulling, Ulf Blanke, and Bernt Schiele. A tutorial on human activity recognition using body-worn inertial sensors. *ACM Comput.Surv. (CSUR)*, 46(3):1–33, Jan. 2014.

[6] Ricardo Chavarriaga, Hesam Sagha, Alberto Calatroni, Sundara Tejaswi Digumarti, Gerhard Tröster, José del R Millán, and Daniel Roggen. The opportunity challenge: A benchmark database for on-body sensor-based activity recognition. *Pattern Recognit. Lett.*, 34(15):2033–2042, Nov. 2013.

[7] Kaixuan Chen, Dalin Zhang, Lina Yao, Bin Guo, Zhiwen Yu, and Yunhao Liu. Deep learning for sensor-based human activity recognition: Overview, challenges, and opportunities. *ACM Comput. Surv. (CSUR)*, 54(4):1–40, May 2021.

[8] Ling Chen, Yingsong Luo, Liangying Peng, Rong Hu, Yi Zhang, and Shenghuan Miao. A multi-graph convolutional network based wearable human activity recognition method using multi-sensors. *Appl. Intell.*, 53(23):28169–28185, 2023.

[9] Yuqing Chen and Yang Xue. A deep learning approach to human activity recognition based on single accelerometer. In *Proc. IEEE Int. Conf. Syst., Man, Cybern.*, pages 1488–1492. IEEE, Oct. 2015.

[10] L Minh Dang, Kyungbok Min, Hanxiang Wang, Md Jalil Piran, Cheol Hee Lee, and Hyeonjoon Moon. Sensor-based and vision-based human activity recognition: A comprehensive survey. *Pattern Recognit.*, 108:Art. no. 107561, Dec. 2020.

[11] Joseph Early, Gavin Cheung, Kurt Cutajar, Hanting Xie, Jas Kandola, and Niall Twomey. Inherently interpretable time series classification via multiple instance learning. In *Proc. Int. Conf. Learn. Repr. (ICLR)*, 2024.

[12] Hassan Ismail Fawaz, Germain Forestier, Jonathan Weber, Lhassane Idoumghar, and Pierre-Alain Muller. Deep learning for time series classification: a review. *Data Mining Knowl. Discov.*, 33(4):917–963, Mar. 2019.

[13] Biswarup Ganguly, Avishek Ghosal, Anirbed Das, Debanjan Das, Debanjan Chatterjee, and Debmalya Rakshit. Automated detection and classification of arrhythmia from ecg signals using feature-induced long short-term memory network. *IEEE Sens. Lett.*, 4(8):1–4, 2020.

[14] Wenbin Gao, Lei Zhang, Wenbo Huang, Fuhong Min, Jun He, and Aiguo Song. Deep neural networks for sensor-based human activity recognition using selective kernel convolution. *IEEE Trans. Instrum. Meas.*, 70:1–13, Aug. 2021.

[15] Jonas Gehring, Michael Auli, David Grangier, Denis Yarats, and Yann N Dauphin. Convolutional sequence to sequence learning. In *International Conference on Machine Learning*, pages 1243–1252. PMLR, 2017.

[16] Ary L Goldberger, Luis AN Amaral, Leon Glass, Jeffrey M Hausdorff, Plamen Ch Ivanov, Roger G Mark, Joseph E Mietus, George B Moody, Chung-Kang Peng, and H Eugene Stanley. Physiobank, physiotoolkit, and physionet: components of a new research resource for complex physiologic signals. *Circulation*, 101(23):e215–e220, 2000.

[17] Nils Y Hammerla, Shane Halloran, and Thomas Plötz. Deep, convolutional, and recurrent models for human activity recognition using wearables. In *Int. Jt. Conf. Artif. Intell. (IJCAI)*, pages 1533–1540, 2016.

[18] Tong He, Zhi Zhang, Hang Zhang, Zhongyue Zhang, Junyuan Xie, and Mu Li. Bag of tricks for image classification with convolutional neural networks. In *Proc. IEEE/CVF Conf. Comput. Vis. Pattern Recognit. (CVPR)*, pages 558–567, Jun. 2019.

[19] Gao Huang, Zhuang Liu, Laurens Van Der Maaten, and Kilian Q Weinberger. Densely connected convolutional networks. In *Proc. IEEE Conf. Comput. Vis. Pattern Recognit. (CVPR)*, pages 4700–4708, Jul. 2017.

[20] Wenbo Huang, Lei Zhang, Wenbin Gao, Fuhong Min, and Jun He. Shallow convolutional neural networks for human activity recognition using wearable sensors. *IEEE Trans. Instrum. Meas.*, 70:1–11, Jun. 2021.

[21] Altaf Hussain, Tanveer Hussain, Waseem Ullah, and Sung Wook Baik. Vision transformer and deep sequence learning for human activity recognition in surveillance videos. *Comput. Intell. Neurosci.*, 2022:Art. no. 3454167, Apr. 2022.

[22] Forrest N. Iandola, Song Han, Matthew W. Moskewicz, Khalid Ashraf, William J. Dally, and Kurt Keutzer. Squeezenet: Alexnet-level accuracy with 50x fewer parameters and $<$0.5mb model size. *arXiv:1602.07360*, 2016.

[23] Andrey Ignatov. Real-time human activity recognition from accelerometer data using convolutional neural networks. *Appl. Soft Comput.*, 62:915–922, Jan. 2018.

[24] Shaik Jameer and Hussain Syed. Deep se-bilstm with ifpoa fine-tuning for human activity recognition using mobile and wearable sensors. *Sensors*, 23(9):4319, 2023.

[25] Wenchao Jiang and Zhaozheng Yin. Human activity recognition using wearable sensors by deep convolutional neural networks. In *Proc. 23rd ACM Int. Conf. Multimedia*, pages 1307–1310, Oct. 2015.

[26] Diederik P Kingma and Jimmy Ba. Adam: A method for stochastic optimization. In *Proc. Int. Conf. Learn. Repr. (ICLR)*, pages 1–15, Jan. 2015.

[27] Chen-Yu Lee, Saining Xie, Patrick Gallagher, Zhengyou Zhang, and Zhuowen Tu. Deeply-supervised nets. In *Proc. Artif. intell. Statist. (AISTATS)*, pages 562–570. PMLR, May 2015.

[28] Athanasios Lentzas and Dimitris Vrakas. Non-intrusive human activity recognition and abnormal behavior detection on elderly people: A review. *Artif. Intell. Rev.*, 53(3):1975–2021, Jun. 2020.

[29] Sachin Mehta and Mohammad Rastegari. Mobilevit: Light-weight, general-purpose, and mobile-friendly vision transformer. In *Proc. Int. Conf. Learn. Repr. (ICLR)*, 2022.

[30] Daniela Micucci, Marco Mobilio, and Paolo Napoletano. Unimib shar: A dataset for human activity recognition using acceleration data from smartphones. *Appl. Sci.*, 7(10):Art. no. 1101, Oct. 2017.

[31] Tomáš Mikolov et al. Statistical language models based on neural networks. *Presented at Google, Mountain View, 2nd Apr.*, 80(26), 2012.

[32] Taima Rahman Mim, Maliha Amatullah, Sadia Afreen, Mohammad Abu Yousuf, Shahadat Uddin, Salem A Alyami, Khondokar Fida Hasan, and Mohammad Ali Moni. GRU-INC: An inception-attention based approach using gru for human activity recognition. *Expert Syst. Appl.*, 216:Art. no. 119419, Apr. 2023.

[33] Mark Nutter, Catherine H Crawford, and Jorge Ortiz. Design of novel deep learning models for real-time human activity recognition with mobile phones. In *Proc. IEEE Int. Joint Conf. Neural Netw. (IJCNN)*, pages 1–8. IEEE, Jul. 2018.

[34] Henry Friday Nweke, Ying Wah Teh, Mohammed Ali Al-Garadi, and Uzoma Rita Alo. Deep learning algorithms for human activity recognition using mobile and wearable sensor networks: State of the art and research challenges. *Expert Syst. Appl.*, 105:233–261, Sep. 2018.

[35] Francisco Javier Ordóñez and Daniel Roggen. Deep convolutional and lstm recurrent neural networks for multimodal wearable activity recognition. *Sensors*, 16(1):Art. no. 115, Jan. 2016.

[36] Jaegyun Park, Won-Seon Lim, Dae-Won Kim, and Jaesung Lee. Multitemporal sampling module for real-time human activity recognition. *IEEE Access*, 10:54507–54515, May 2022.

[37] Jaegyun Park, Won-Seon Lim, Dae-Won Kim, and Jaesung Lee. GTSNet: Flexible architecture under budget constraint for real-time human activity recognition from wearable sensor. *Eng. Appl. Artif. Intell.*, 124:Art. no. 106543, Sep. 2023.

[38] Adam Paszke, Sam Gross, Francisco Massa, Adam Lerer, James Bradbury, Gregory Chanan, Trevor Killeen, Zeming Lin, Natalia Gimelshein, Luca Antiga, et al. Pytorch: An imperative style, high-performance deep learning library. In *Proc. Adv. Neural Inf. Proces. Syst. (NIPS)*, volume 32, pages 8026–8037, 2019.

[39] Bach-Tung Pham, Phuong Thi Le, Tzu-Chiang Tai, Yi-Chiung Hsu, Yung-Hui Li, and Jia-Ching Wang. Electrocardiogram heartbeat classification for arrhythmias and myocardial infarction. *Sensors*, 23(6):2993, 2023.

[40] Rishav Pramanik, Ritodeep Sikdar, and Ram Sarkar. Transformer-based deep reverse attention network for multi-sensory human activity recognition. *Eng. Appl. Artif. Intell.*, 122:106150, Jun. 2023.

[41] Andrea Prati, Caifeng Shan, and Kevin I-Kai Wang. Sensors, vision and networks: From video surveillance to activity recognition and health monitoring. *J. Ambient Intell. Smart Environ.*, 11 (1):5–22, Jan. 2019.

[42] Jun Qi, Po Yang, Atif Waraich, Zhikun Deng, Youbing Zhao, and Yun Yang. Examining sensor-based physical activity recognition and monitoring for healthcare using internet of things: A systematic review. *J. Biomed. Informat.*, 87:138–153, 2018.

[43] Sen Qiu, Hongkai Zhao, Nan Jiang, Zhelong Wang, Long Liu, Yi An, Hongyu Zhao, Xin Miao, Ruichen Liu, and Giancarlo Fortino. Multi-sensor information fusion based on machine learning for real applications in human activity recognition: State-of-the-art and research challenges. *Inf. Fusion*, 80:241–265, Apr. 2022.

[44] E Ramanujam, Thinagaran Perumal, and S Padmavathi. Human activity recognition with smartphone and wearable sensors using deep learning techniques: A review. *IEEE Sensors J.*, 21(12):13029–13040, Mar. 2021.

[45] Daniele Ravi, Charence Wong, Benny Lo, and Guang-Zhong Yang. A deep learning approach to on-node sensor data analytics for mobile or wearable devices. *IEEE J. Biomed. Health Informat.*, 21(1):56–64, Dec. 2016.

[46] Attila Reiss and Didier Stricker. Introducing a new benchmarked dataset for activity monitoring. In *Proc. IEEE 16th Int. Symp. Wearable Comput. (ISWC)*, pages 108–109. IEEE, Jun. 2012.

[47] Niloy Sikder and Abdullah-Al Nahid. Ku-har: An open dataset for heterogeneous human activity recognition. *Pattern Recognit. Lett.*, 146:46–54, Jun. 2021.

[48] Yin Tang, Lei Zhang, Fuhong Min, and Jun He. Multiscale deep feature learning for human activity recognition using wearable sensors. *IEEE Trans. Ind. Electron.*, 70(2):2106–2116, Mar. 2022.

[49] Qi Teng, Yin Tang, and Guangwei Hu. Rephar: Decoupling networks with accuracy-speed tradeoff for sensor-based human activity recognition. *IEEE Trans. Instrum. Meas.*, 72:1–11, Feb. 2023.

[50] Lina Tong, Hanghang Ma, Qianzhi Lin, Jiaji He, and Liang Peng. A novel deep learning bi-gru-i model for real-time human activity recognition using inertial sensors. *IEEE Sensors J.*, 22(6): 6164–6174, Feb. 2022.

[51] Shaohua Wan, Lianyong Qi, Xiaolong Xu, Chao Tong, and Zonghua Gu. Deep learning models for real-time human activity recognition with smartphones. *Mob. Netw. Appl.*, 25(2):743–755, Dec. 2020.

[52] Jindong Wang, Yiqiang Chen, Shuji Hao, Xiaohui Peng, and Lisha Hu. Deep learning for sensor-based activity recognition: A survey. *Pattern Recognit. Lett.*, 119:3–11, Mar. 2019.

[53] Yan Wang, Shuang Cang, and Hongnian Yu. A survey on wearable sensor modality centred human activity recognition in health care. *Expert Syst. Appl.*, 137:167–190, Dec. 2019.

[54] Zhiguang Wang, Weizhong Yan, and Tim Oates. Time series classification from scratch with deep neural networks: A strong baseline. In *Proc. IEEE Int. Joint Conf. Neural Netw. (IJCNN)*, pages 1578–1585. IEEE, May 2017.

[55] Qiao Xiao, Boqian Wu, Yu Zhang, Shiwei Liu, Mykola Pechenizkiy, Elena Mocanu, and Decebal Constantin Mocanu. Dynamic sparse network for time series classification: Learning what to "see". *Proc. Adv. Neural Inf. Proces. Syst. (NeurIPS)*, 35:16849–16862, 2022.

[56] Cheng Xu, Duo Chai, Jie He, Xiaotong Zhang, and Shihong Duan. Innohar: A deep neural network for complex human activity recognition. *IEEE Access*, 7:9893–9902, Jan. 2019.

[57] Qi Xu, Ming Zhang, Zonghua Gu, and Gang Pan. Overfitting remedy by sparsifying regularization on fully-connected layers of cnns. *Neurocomputing*, 328:69–74, Feb. 2019.

[58] Fisher Yu, Dequan Wang, Evan Shelhamer, and Trevor Darrell. Deep layer aggregation. In *Proc. IEEE Conf. Comput. vis. Pattern Recognit. (CVPR)*, pages 2403–2412, 2018.

[59] Afia Zafar, Muhammad Aamir, Nazri Mohd Nawi, Ali Arshad, Saman Riaz, Abdulrahman Alruban, Ashit Kumar Dutta, and Sultan Almotairi. A comparison of pooling methods for convolutional neural networks. *Appl. Sci.*, 12(17):8643, 2022.

[60] Tahmina Zebin, Patricia J Scully, Niels Peek, Alexander J Casson, and Krikor B Ozanyan. Design and implementation of a convolutional neural network on an edge computing smartphone for human activity recognition. *IEEE Access*, 7:133509–133520, Sep. 2019.

[61] Shibo Zhang, Yaxuan Li, Shen Zhang, Farzad Shahabi, Stephen Xia, Yu Deng, and Nabil Alshurafa. Deep learning in human activity recognition with wearable sensors: A review on advances. *Sensors*, 22(4):Art. no. 1476, Feb. 2022.

[62] Xiangyu Zhang, Xinyu Zhou, Mengxiao Lin, and Jian Sun. Shufflenet: An extremely efficient convolutional neural network for mobile devices. In *Proc. IEEE Conf. Comput. Vis. Pattern Recognit. (CVPR)*, pages 6848–6856, Jun. 2018.

[63] Ye Zhang, Longguang Wang, Huiling Chen, Aosheng Tian, Shilin Zhou, and Yulan Guo. If-convtransformer: A framework for human activity recognition using imu fusion and convtransformer. *Proc. ACM Interact. Mob. Wearable Ubiquitous Technol.*, 6(2):1–26, Jul. 2022.

[64] Bowen Zhao, Huanlai Xing, Xinhan Wang, Fuhong Song, and Zhiwen Xiao. Rethinking attention mechanism in time series classification. *Inf. Sci.*, 627:97–114, 2023.

Appendix

A Proof of Proposition 1

Given the original signals $X^{(0)} \in \mathbb{R}^{\mathbb{T},\mathbb{M}}$, the first convolution layer generates new feature signals $X^{(1)} \in \mathbb{R}^{\mathbb{T},N^1}$, resulting in a time complexity of $\mathcal{O}(\mathbb{T}\mathbb{M}N^{(1)}D_k^{(1)})$. Suppose that the l-th intermediate convolution layer includes a kernel $K^{(l)} \in \mathbb{R}^{D_k^{(l)},N^{(l-1)},N^{(l)}}$ and $N^{(l)}$ is a positive-integer multiple of $N^{(l-1)}$, that is, $N^{(l)} = c^{(l)}N^{(l-1)}$. Generally, $c \geq 1$ and the pooling layer adjusts the temporal resolution T to T/c if $c \geq 2$. Therefore, its time complexity is $\mathcal{O}(T^{(l)}D_k^{(l)}M^{(l)}N^{(l)})) = \mathcal{O}(T^{(l-1)}D_k^{(l)}(N^{(l-1)})^2)$. Given the stack of L convolution layers, their time complexity can be simplified as follows:

$$\underbrace{\mathcal{O}(\mathbb{T}\mathbb{D}_k\mathbb{M}\mathbb{N})}_{\textit{Part 1}} + \mathcal{O}(\mathbb{T}\mathbb{D}_k\mathbb{N}^2 L), \tag{10}$$

where $\mathbb{N}$ and $\mathbb{D}_k$ are the average of the number of output features and the kernel sizes across the layers, respectively. If $\mathbb{M} \leq \mathbb{N}(L-1)$, the time complexity of convolution layers becomes $\mathcal{O}(\mathbb{T}\mathbb{D}_k\mathbb{N}^2 L)$.

B Proof of Lemma 1

Consistent with Proposition 1, the time complexity of calculating the features is $\mathcal{O}(\mathbb{T}\mathbb{D}_k\mathbb{N}^2 L)$. Since the number of output channels across the standard convolution layers is $\mathbb{N}$, the time complexity of calculating LCTMs for all layers is $\mathcal{O}(\mathbb{T}\mathbb{N}^2 L)$. Given $L \times \mathbb{N}$ aggregated features and V activities, the Softmax layer predicts an activity with the time complexity of $\mathcal{O}(L\mathbb{N}V)$. Consequently, the time complexity of our CALANet is formalized as:

$$\underbrace{\mathcal{O}(\mathbb{T}\mathbb{D}_k\mathbb{N}^2 L)}_{\textit{Part 2}} + \underbrace{\mathcal{O}(\mathbb{T}\mathbb{N}^2 L)}_{\textit{Part 3}} + \underbrace{\mathcal{O}(L\mathbb{N}V)}_{\textit{Part 4}}. \tag{11}$$

Because V commonly is less than $\mathbb{T} \times \mathbb{D}_k \times \mathbb{N}$, Eq. (11) can be rewritten as $\mathcal{O}(\mathbb{T}\mathbb{D}_k\mathbb{N}^2 L)$.

C Proof of Lemma 2

Given an input $X \in \mathbb{R}^{T,M}$, M channels are evenly divided into L channel groups. More precisely, for each channel group, the convolution layer generates $\lfloor N/L \rfloor$ output channels, resulting in the time complexity of $\mathcal{O}(TD_k(MN/L^2))$. Since each convolution layer generates the output $Y \in \mathbb{R}^{T,N}$ across L channel groups, the time complexity of each layer is $\mathcal{O}(TD_k(MN/L))$. Because our CALANet includes L standard convolution layers to calculate the local temporal correlations, part 2 of Eq. (11) is reduced to $\mathcal{O}(\mathbb{T}\mathbb{D}_k\mathbb{N}^2)$, consistent with Proposition 1.

D Proof of Lemma 3

Given an input $X \in \mathbb{R}^{T,M}$, LCTMs at each layer generate a vector with $\lfloor \mathbb{N}/L \rfloor$ elements, resulting in the time complexity of $\mathcal{O}(TM(\mathbb{N}/L))$. As shown in Figure 2, the number of output channels for each layer is fixed as $\mathbb{N}$ across layers. Therefore, the time complexity of the all-layer aggregation is $\mathcal{O}(T(\mathbb{N}^2/L))$. Similar to Lemma 2, part 3 of Eq. (11) is reduced to $\mathcal{O}(\mathbb{T}\mathbb{N}^2)$.

E Proof of Theorem 1

Consistent with Lemma 2 and Lemma 3, part 2 and part 3 of Eq. (11) is simplified as:

$$\mathcal{O}(\mathbb{T}\mathbb{D}_k\mathbb{N}^2) + \mathcal{O}(\mathbb{T}\mathbb{N}^2) \tag{12}$$

In addition, we fixed the number of features fed into the Softmax layer to $\mathbb{N}$. Therefore, part 4 of Eq. (11) is reduced to $\mathcal{O}(\mathbb{N}V)$. Because V commonly is less than $\mathbb{T} \times \mathbb{D}_k \times \mathbb{N}$, Eq. (6) is reduced $\mathcal{O}(\mathbb{T}\mathbb{D}_k\mathbb{N}^2)$.

F Details of datasets

The benchmark datasets used in our experiment follow the following setup:

- The **UCI-HAR** dataset [1] was recorded at a sampling frequency of 50 Hz. Precisely, 30 subjects performed six basic activities (e.g., walking, upstairs, sitting) using accelerometers and gyroscopes embedded in Android smartphones. As the authors recommended, each segment's length is set to 128, and 70% and 30% of the dataset were used as the training and test sets, respectively.
- The **UniMiB-SHAR** dataset [30] was recorded at a sampling frequency of 50 Hz, where the length of each segment is 151. The 30 subjects performed 17 activities, including nine activities of daily living (e.g., walking and standing) and eight fall activities (e.g., forward and syncope), using an accelerometer in Android smartphones. Precisely, 70% and 30% of the dataset were used as the training and test sets, respectively.
- The **DSADS** dataset [3] was recorded at a sampling frequency of 25 Hz, where the length of each segment is 125. Eight subjects performed 19 daily and sports activities (e.g., exercising on a stepper and rowing) using accelerometers, gyroscopes, and magnetometers embedded in five MTx trackers. More precisely, the MTx units measured the sensor signals on the torso, right arm, left arm, right leg, and left leg. We split the dataset into 80% training and 20% test sets based on the subject's identification (ID).
- The **OPPORTUNITY** dataset [6] was recorded at a sampling frequency of 30 Hz in a sensor-rich environment with wearable, object, and ambient sensors, where the length of each segment is 90. We only considered wearable sensors for real-time HAR, including accelerometers and inertial measurement units (IMUs); the number of input channels is 113 in our experiments. The four subjects performed 17 activities, including complicated activities such as "drink from cup" and "open door," categorized into ADL 1-5 and Drill. We used the ADL 5 data for subject 1; the Drill data for subject 2; the ADL 1 and 4 data for subject 3; and the ADL 4 data for subject 4 as the test set [32]. The remaining data were used as the training set.
- The **KU-HAR** dataset [47] was recorded at a sampling frequency of 100 Hz, where the length of each segment is 300. Precisely, 90 subjects performed 18 daily activities (e.g., talking with hand movements and picking up an abject) using accelerometers and gyroscopes embedded in smartphones. The 80% and 20% of the dataset were used as the training and test sets, respectively.
- The **PAMAP2** dataset [46] was recorded at 100 and 9 Hz sampling frequencies for IMUs and a heart rate monitor, respectively. Precisely, nine subjects performed 18 activities, including basic activities (e.g., sitting and running) and complicated activities (e.g., watching TV and folding laundry), where the length of each segment is 512. We used the data aggregated from subjects 102 and 106 as the test set. In addition, we added 30% of the data for "watching TV", "car driving," and "playing soccer" into the test set because they were performed by only one subject. The remaining data were used as the training set.
- The **REALDISP** dataset [2] was recorded at a sampling frequency of 50 Hz from nine IMUs, where the length of each segment is 250. More precisely, 17 subjects performed 33 fitness activities (e.g., lateral bend arm up and upper trunk and lower body opposite twist) using accelerometers, gyroscopes, and magnetometers. In addition, the authors provided orientation estimates in quaternion format. We split the dataset into 70% training and 30% test sets based on subject ID.

G Details of baselines

We summarize the models used in our experiments, as follows:

- **CNNs for real-time HAR.** We adopted three CNNs as state-of-the-art models in real-time HAR. Shallow ConvNet [23] comprises a single convolution layer and two fully-connected layers, where the basic statistical features to encode global temporal information are concatenated with outputs of the convolution layer. RepHAR [49] comprises three convolution layers with re-parameterization and a Softmax layer. Res-GTSNet [37] contains nine grouped temporal shift module layers and a Softmax layer.

- **CNNs with recurrent layers or attention mechanisms.** We adopted two CNNs with recurrent layers and two CNNs with attention mechanisms to verify the effectiveness of our all-layer aggregation. DeepConvLSTM [35] contains four convolution layers and two recurrent LSTM layers with a Softmax classifier. Bi-GRU-I [50] is composed of two bi-directional GRU layers, three inception layers, and a Softmax layer. Compared with DeepConvLSTM, its architecture has a reverse order of convolution and recurrent layers. RevAttNet [40] contains six convolutional layers, two recurrent layers, and two reverse attention modules, including LSTM, deconvolution, and multi-head attention. IF-ConvTransformer [63] is composed of IMU fusion blocks, four convolutional layers, and two self-attention layers, where the IMU fusion blocks are used to fuse the features from multiple sensor modalities based on sensor-wise convolutional layers.

- **Time-Series Classification (TSC) models.** In addition, we adopted two CNNs that achieved substantial success in the TSC, which is more general-purpose than HAR. Specifically, T-ResNet [54, 12] consists of three residual blocks, each comprising three convolution layers with a residual connection, and a Softmax layer. T-FCN [54, 12] consists of three convolution layers and a Softmax layer. Compared with the real-time models, it has more output channels. MILLET [11] comprises five identical networks with conjunctive pooling layers, where each network contains six convolutional layers with multiple kernel sizes. DSN [55] contains three sparse CNN module, each of which includes a dynamic sparse convolution and point-wise convolution.

For fairness, we re-implemented all the baseline networks in PyTorch [38] and excluded sophisticated tricks of each original setting, such as a gradient clipping [31] and learning rate warmup [18]. Precisely, they were trained for 300 epochs with a batch size of 128 using a 2080Ti graphics-processing unit. We used the Adam optimizer [26] with $\beta_1 = 0.9$, $\beta_2 = 0.999$ and $\epsilon = 10^{-8}$, where the learning rate and weight decay were set to 0.0005. For the CALALet, we set $\mathbb{D}_k$, $\mathbb{N}$, and L to 5, 128, and 9, respectively. On the OPPORTUNITY and REALDISP datasets with many input channels (113 and 117), we doubled the number of filters for the first convolution of CALANet. The hyper-parameters of the existing networks are set according to the values recommended in the original papers.

H Confusion matrices

Figures 5–7 show the confusion matrices of CALANet on three datasets. Their diagonal elements represent the number of instances correctly classified to the related activities, with the color darkening as the number grows.

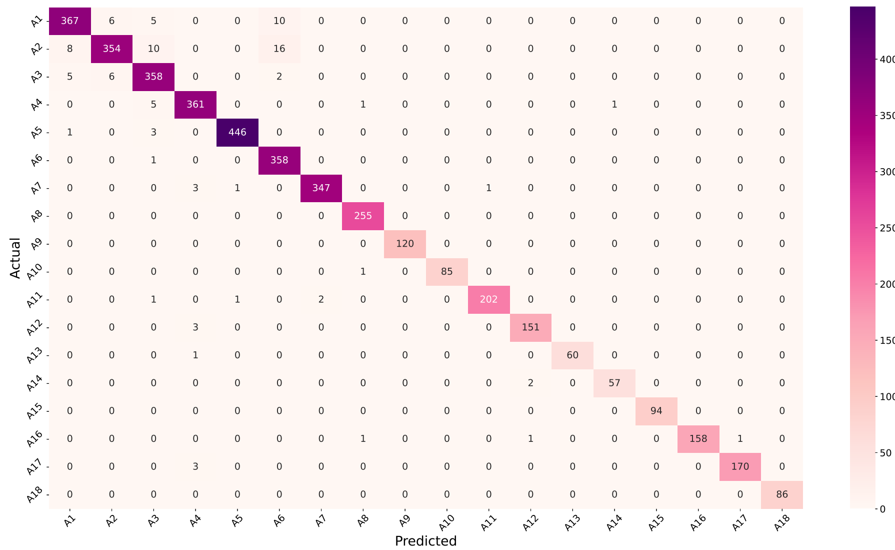

Figure 5: Confusion matrix of CALANet on the KU-HAR dataset. A1, stand; A2, sit; A3, talk-sit; A4, talk-stand; A5, stand-sit; A6, lay; A7, lay-stand; A8, pick; A9, jump; A10, push-up; A11, sit-up; A12, walk; A13, walk-backward; A14, walk-circle; A15, run; A16, stair-up; A17, stair-down; A18, table-tennis.

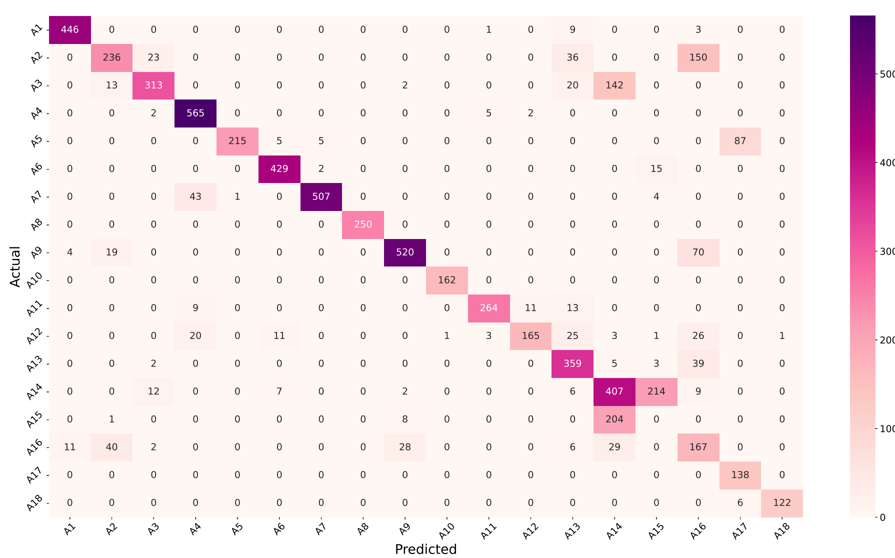

Figure 6: Confusion matrix of CALANet on the PAMAP2 dataset. A1, lying; A2, sitting; A3, standing; A4, walking; A5, running; A6, cycling; A7, Nordic-walking; A8, watching-TV; A9, computer-work; A10, car-driving; A11, ascending-stairs; A12, descending-stairs; A13, vacuum-cleaning; A14, ironing; A15, folding-laundry; A16, house-cleaning; A17, playing-soccer; A18, rope-jumping.

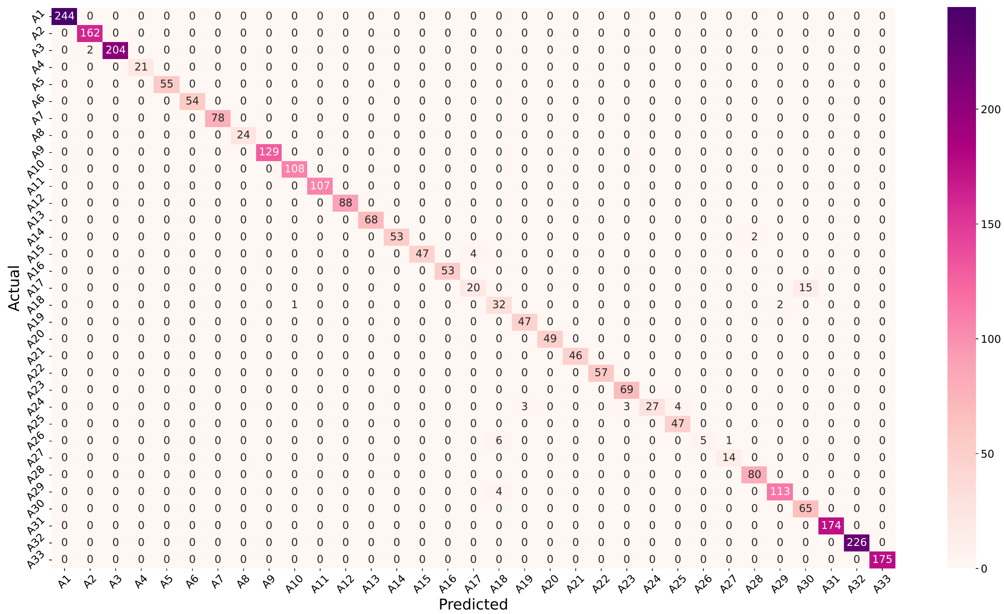

Figure 7: Confusion matrix of CALANet on the REALDISP dataset. A1, walking; A2, jogging; A3, running; A4, jump-up; A5, jump-front-back; A6, jump-sideways; A7, jump-leg/arms-open/closed; A8, jump-rope; A9, trunk-twist-arms; A10, trunk-twist-elbows; A11, waist-bends-forward; A12, waist-rotation; A13, waist-bends; A14, reach-heels-backwards; A15, lateral-bend; A16, lateral-bend-arm-up; A17, repetitive-forward-stretching; A18, upper-trunk-and-lower-body-opposite-twist; A19, arms-lateral-elevation; A20, arms-frontal-elevation; A21, frontal-hand-claps; A22, arms-frontal-crossing; A23, shoulders-high-amplitude-rotation; A24, shoulders-low-amplitude-rotation; A25, arms-inner-rotation; A26, knees-alternatively-breast; A27, heels-alternatively-backside; A28, knees-bending-crouching; A29, knees-alternatively-bend-forward; A30, rotation-on-the-knees; A31, rowing; A32, elliptical-bike; A33, cycling.

I ECG heartbeat classification

We applied CALANet to the ECG heartbeat classification problem using the MIT-BIH arrhythmia dataset [16], which includes 24-hour ambulatory ECG recordings collected from inpatients and outpatients at Boston's Beth Israel Hospital. The dataset has 21,892 heartbeats, each with a signal length of 187. In Table 6, CALANet exhibited comparable performance with other networks designed to process ECG signals. This result shows that CALANet has promising applicability to other ML applications.

Table 6: Comparison results on the MIT-BIH arrhythmia dataset.

Model	Average Accuracy
CALANet	98.2
Pham et al. [39]	98.5
Ganguly et al. [13]	97.3

NeurIPS Paper Checklist

1. **Claims**

   Question: Do the main claims made in the abstract and introduction accurately reflect the paper's contributions and scope?

   Answer: [Yes]

   Justification: To achieve real-time HAR, prior HAR studies designed the network architectures of CNNs by restricting the number of layers shallowly or reducing connections of each layer, resulting in the significant loss of accuracy. The proposed method addressed this problem by improving the accuracy based on cheap all-layer aggregation while maintaining the computational cost of the existing real-time HAR networks.

   Guidelines:

   - The answer NA means that the abstract and introduction do not include the claims made in the paper.
   - The abstract and/or introduction should clearly state the claims made, including the contributions made in the paper and important assumptions and limitations. A No or NA answer to this question will not be perceived well by the reviewers.
   - The claims made should match theoretical and experimental results, and reflect how much the results can be expected to generalize to other settings.
   - It is fine to include aspirational goals as motivation as long as it is clear that these goals are not attained by the paper.

2. **Limitations**

   Question: Does the paper discuss the limitations of the work performed by the authors?

   Answer: [Yes]

   Justification: This paper does not consider various computational budgets that may be changed according to the specific devices. This limitation must be improved via future works such as neural architecture search, runtime optimization, and parallel computation.

   Guidelines:

   - The answer NA means that the paper has no limitation while the answer No means that the paper has limitations, but those are not discussed in the paper.
   - The authors are encouraged to create a separate "Limitations" section in their paper.
   - The paper should point out any strong assumptions and how robust the results are to violations of these assumptions (e.g., independence assumptions, noiseless settings, model well-specification, asymptotic approximations only holding locally). The authors should reflect on how these assumptions might be violated in practice and what the implications would be.
   - The authors should reflect on the scope of the claims made, e.g., if the approach was only tested on a few datasets or with a few runs. In general, empirical results often depend on implicit assumptions, which should be articulated.
   - The authors should reflect on the factors that influence the performance of the approach. For example, a facial recognition algorithm may perform poorly when image resolution is low or images are taken in low lighting. Or a speech-to-text system might not be used reliably to provide closed captions for online lectures because it fails to handle technical jargon.
   - The authors should discuss the computational efficiency of the proposed algorithms and how they scale with dataset size.
   - If applicable, the authors should discuss possible limitations of their approach to address problems of privacy and fairness.
   - While the authors might fear that complete honesty about limitations might be used by reviewers as grounds for rejection, a worse outcome might be that reviewers discover limitations that aren't acknowledged in the paper. The authors should use their best judgment and recognize that individual actions in favor of transparency play an important role in developing norms that preserve the integrity of the community. Reviewers will be specifically instructed to not penalize honesty concerning limitations.

3. **Theory Assumptions and Proofs**

   Question: For each theoretical result, does the paper provide the full set of assumptions and a complete (and correct) proof?

   Answer: [Yes]

   Justification: We proved that the computational cost of CALANet is equivalent to that of conventional CNNs, including shallow networks.

   Guidelines:

   - The answer NA means that the paper does not include theoretical results.
   - All the theorems, formulas, and proofs in the paper should be numbered and cross-referenced.
   - All assumptions should be clearly stated or referenced in the statement of any theorems.
   - The proofs can either appear in the main paper or the supplemental material, but if they appear in the supplemental material, the authors are encouraged to provide a short proof sketch to provide intuition.
   - Inversely, any informal proof provided in the core of the paper should be complemented by formal proofs provided in appendix or supplemental material.
   - Theorems and Lemmas that the proof relies upon should be properly referenced.

4. **Experimental Result Reproducibility**

   Question: Does the paper fully disclose all the information needed to reproduce the main experimental results of the paper to the extent that it affects the main claims and/or conclusions of the paper (regardless of whether the code and data are provided or not)?

   Answer: [Yes]

   Justification: We will release our code by including the GitHub link in the paper if finishing the blind review process.

   Guidelines:

   - The answer NA means that the paper does not include experiments.
   - If the paper includes experiments, a No answer to this question will not be perceived well by the reviewers: Making the paper reproducible is important, regardless of whether the code and data are provided or not.
   - If the contribution is a dataset and/or model, the authors should describe the steps taken to make their results reproducible or verifiable.
   - Depending on the contribution, reproducibility can be accomplished in various ways. For example, if the contribution is a novel architecture, describing the architecture fully might suffice, or if the contribution is a specific model and empirical evaluation, it may be necessary to either make it possible for others to replicate the model with the same dataset, or provide access to the model. In general. releasing code and data is often one good way to accomplish this, but reproducibility can also be provided via detailed instructions for how to replicate the results, access to a hosted model (e.g., in the case of a large language model), releasing of a model checkpoint, or other means that are appropriate to the research performed.
   - While NeurIPS does not require releasing code, the conference does require all submissions to provide some reasonable avenue for reproducibility, which may depend on the nature of the contribution. For example
     (a) If the contribution is primarily a new algorithm, the paper should make it clear how to reproduce that algorithm.
     (b) If the contribution is primarily a new model architecture, the paper should describe the architecture clearly and fully.
     (c) If the contribution is a new model (e.g., a large language model), then there should either be a way to access this model for reproducing the results or a way to reproduce the model (e.g., with an open-source dataset or instructions for how to construct the dataset).
     (d) We recognize that reproducibility may be tricky in some cases, in which case authors are welcome to describe the particular way they provide for reproducibility.

In the case of closed-source models, it may be that access to the model is limited in some way (e.g., to registered users), but it should be possible for other researchers to have some path to reproducing or verifying the results.

5. **Open access to data and code**

   Question: Does the paper provide open access to the data and code, with sufficient instructions to faithfully reproduce the main experimental results, as described in supplemental material?

   Answer: [Yes]

   Justification: We will release our code by including the GitHub link in the paper if finishing the blind review process.

   Guidelines:

   - The answer NA means that paper does not include experiments requiring code.
   - Please see the NeurIPS code and data submission guidelines (`https://nips.cc/public/guides/CodeSubmissionPolicy`) for more details.
   - While we encourage the release of code and data, we understand that this might not be possible, so "No" is an acceptable answer. Papers cannot be rejected simply for not including code, unless this is central to the contribution (e.g., for a new open-source benchmark).
   - The instructions should contain the exact command and environment needed to run to reproduce the results. See the NeurIPS code and data submission guidelines (`https://nips.cc/public/guides/CodeSubmissionPolicy`) for more details.
   - The authors should provide instructions on data access and preparation, including how to access the raw data, preprocessed data, intermediate data, and generated data, etc.
   - The authors should provide scripts to reproduce all experimental results for the new proposed method and baselines. If only a subset of experiments are reproducible, they should state which ones are omitted from the script and why.
   - At submission time, to preserve anonymity, the authors should release anonymized versions (if applicable).
   - Providing as much information as possible in supplemental material (appended to the paper) is recommended, but including URLs to data and code is permitted.

6. **Experimental Setting/Details**

   Question: Does the paper specify all the training and test details (e.g., data splits, hyperparameters, how they were chosen, type of optimizer, etc.) necessary to understand the results?

   Answer: [Yes]

   Justification: The full details are provided in the code and appendix.

   Guidelines:

   - The answer NA means that the paper does not include experiments.
   - The experimental setting should be presented in the core of the paper to a level of detail that is necessary to appreciate the results and make sense of them.
   - The full details can be provided either with the code, in appendix, or as supplemental material.

7. **Experiment Statistical Significance**

   Question: Does the paper report error bars suitably and correctly defined or other appropriate information about the statistical significance of the experiments?

   Answer: [Yes]

   Justification: We performed a paired t-test at the 95% significance level on each dataset.

   Guidelines:

   - The answer NA means that the paper does not include experiments.
   - The authors should answer "Yes" if the results are accompanied by error bars, confidence intervals, or statistical significance tests, at least for the experiments that support the main claims of the paper.

- The factors of variability that the error bars are capturing should be clearly stated (for example, train/test split, initialization, random drawing of some parameter, or overall run with given experimental conditions).
- The method for calculating the error bars should be explained (closed form formula, call to a library function, bootstrap, etc.)
- The assumptions made should be given (e.g., Normally distributed errors).
- It should be clear whether the error bar is the standard deviation or the standard error of the mean.
- It is OK to report 1-sigma error bars, but one should state it. The authors should preferably report a 2-sigma error bar than state that they have a 96% CI, if the hypothesis of Normality of errors is not verified.
- For asymmetric distributions, the authors should be careful not to show in tables or figures symmetric error bars that would yield results that are out of range (e.g. negative error rates).
- If error bars are reported in tables or plots, The authors should explain in the text how they were calculated and reference the corresponding figures or tables in the text.

8. **Experiments Compute Resources**

   Question: For each experiment, does the paper provide sufficient information on the computer resources (type of compute workers, memory, time of execution) needed to reproduce the experiments?

   Answer: [Yes]

   Justification: The appendix includes the details on the computer resources.

   Guidelines:

   - The answer NA means that the paper does not include experiments.
   - The paper should indicate the type of compute workers CPU or GPU, internal cluster, or cloud provider, including relevant memory and storage.
   - The paper should provide the amount of compute required for each of the individual experimental runs as well as estimate the total compute.
   - The paper should disclose whether the full research project required more compute than the experiments reported in the paper (e.g., preliminary or failed experiments that didn't make it into the paper).

9. **Code Of Ethics**

   Question: Does the research conducted in the paper conform, in every respect, with the NeurIPS Code of Ethics `https://neurips.cc/public/EthicsGuidelines`?

   Answer: [Yes]

   Justification: This research does NOT violate the the NeurIPS Code of Ethics.

   Guidelines:

   - The answer NA means that the authors have not reviewed the NeurIPS Code of Ethics.
   - If the authors answer No, they should explain the special circumstances that require a deviation from the Code of Ethics.
   - The authors should make sure to preserve anonymity (e.g., if there is a special consideration due to laws or regulations in their jurisdiction).

10. **Broader Impacts**

    Question: Does the paper discuss both potential positive societal impacts and negative societal impacts of the work performed?

    Answer: [Yes]

    Justification: As HAR is a fundamental technique in healthcare, fitness tracking, and surveillance, our accurate and real-time model can reduce the negative societal impacts due to false predictions.

    Guidelines:

    - The answer NA means that there is no societal impact of the work performed.

- If the authors answer NA or No, they should explain why their work has no societal impact or why the paper does not address societal impact.
- Examples of negative societal impacts include potential malicious or unintended uses (e.g., disinformation, generating fake profiles, surveillance), fairness considerations (e.g., deployment of technologies that could make decisions that unfairly impact specific groups), privacy considerations, and security considerations.
- The conference expects that many papers will be foundational research and not tied to particular applications, let alone deployments. However, if there is a direct path to any negative applications, the authors should point it out. For example, it is legitimate to point out that an improvement in the quality of generative models could be used to generate deepfakes for disinformation. On the other hand, it is not needed to point out that a generic algorithm for optimizing neural networks could enable people to train models that generate Deepfakes faster.
- The authors should consider possible harms that could arise when the technology is being used as intended and functioning correctly, harms that could arise when the technology is being used as intended but gives incorrect results, and harms following from (intentional or unintentional) misuse of the technology.
- If there are negative societal impacts, the authors could also discuss possible mitigation strategies (e.g., gated release of models, providing defenses in addition to attacks, mechanisms for monitoring misuse, mechanisms to monitor how a system learns from feedback over time, improving the efficiency and accessibility of ML).

11. **Safeguards**

    Question: Does the paper describe safeguards that have been put in place for responsible release of data or models that have a high risk for misuse (e.g., pretrained language models, image generators, or scraped datasets)?

    Answer: [Yes]

    Justification: We will include the usage guidelines or restrictions in code release.

    Guidelines:

    - The answer NA means that the paper poses no such risks.
    - Released models that have a high risk for misuse or dual-use should be released with necessary safeguards to allow for controlled use of the model, for example by requiring that users adhere to usage guidelines or restrictions to access the model or implementing safety filters.
    - Datasets that have been scraped from the Internet could pose safety risks. The authors should describe how they avoided releasing unsafe images.
    - We recognize that providing effective safeguards is challenging, and many papers do not require this, but we encourage authors to take this into account and make a best faith effort.

12. **Licenses for existing assets**

    Question: Are the creators or original owners of assets (e.g., code, data, models), used in the paper, properly credited and are the license and terms of use explicitly mentioned and properly respected?

    Answer: [Yes]

    Justification: We cited the original paper that produced the datasets and our source code release follows GPL-3.0 license.

    Guidelines:

    - The answer NA means that the paper does not use existing assets.
    - The authors should cite the original paper that produced the code package or dataset.
    - The authors should state which version of the asset is used and, if possible, include a URL.
    - The name of the license (e.g., CC-BY 4.0) should be included for each asset.
    - For scraped data from a particular source (e.g., website), the copyright and terms of service of that source should be provided.

- If assets are released, the license, copyright information, and terms of use in the package should be provided. For popular datasets, `paperswithcode.com/datasets` has curated licenses for some datasets. Their licensing guide can help determine the license of a dataset.
- For existing datasets that are re-packaged, both the original license and the license of the derived asset (if it has changed) should be provided.
- If this information is not available online, the authors are encouraged to reach out to the asset's creators.

13. **New Assets**

    Question: Are new assets introduced in the paper well documented and is the documentation provided alongside the assets?

    Answer: [Yes]

    Justification: The paper and the code release include the details about training, license, usage guidelines, etc.

    Guidelines:

    - The answer NA means that the paper does not release new assets.
    - Researchers should communicate the details of the dataset/code/model as part of their submissions via structured templates. This includes details about training, license, limitations, etc.
    - The paper should discuss whether and how consent was obtained from people whose asset is used.
    - At submission time, remember to anonymize your assets (if applicable). You can either create an anonymized URL or include an anonymized zip file.

14. **Crowdsourcing and Research with Human Subjects**

    Question: For crowdsourcing experiments and research with human subjects, does the paper include the full text of instructions given to participants and screenshots, if applicable, as well as details about compensation (if any)?

    Answer: [NA]

    Justification: We used only public datasets.

    Guidelines:

    - The answer NA means that the paper does not involve crowdsourcing nor research with human subjects.
    - Including this information in the supplemental material is fine, but if the main contribution of the paper involves human subjects, then as much detail as possible should be included in the main paper.
    - According to the NeurIPS Code of Ethics, workers involved in data collection, curation, or other labor should be paid at least the minimum wage in the country of the data collector.

15. **Institutional Review Board (IRB) Approvals or Equivalent for Research with Human Subjects**

    Question: Does the paper describe potential risks incurred by study participants, whether such risks were disclosed to the subjects, and whether Institutional Review Board (IRB) approvals (or an equivalent approval/review based on the requirements of your country or institution) were obtained?

    Answer: [NA]

    Justification: We used only public datasets.

    Guidelines:

    - The answer NA means that the paper does not involve crowdsourcing nor research with human subjects.
    - Depending on the country in which research is conducted, IRB approval (or equivalent) may be required for any human subjects research. If you obtained IRB approval, you should clearly state this in the paper.

- We recognize that the procedures for this may vary significantly between institutions and locations, and we expect authors to adhere to the NeurIPS Code of Ethics and the guidelines for their institution.
- For initial submissions, do not include any information that would break anonymity (if applicable), such as the institution conducting the review.